

RESEARCH ARTICLE | APRIL 23 2024

## Laboratory study of rotationally inelastic collisions of CO<sub>2</sub> at low temperatures

C. Álvarez ; G. Tejada ; J. M. Fernández 

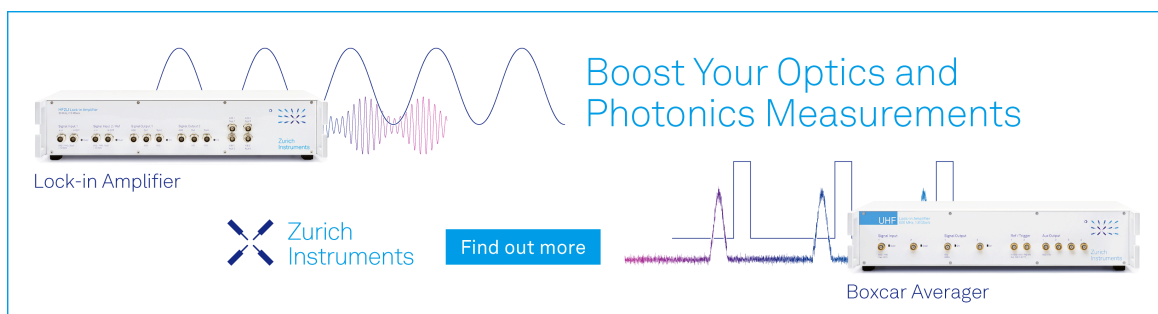


*J. Chem. Phys.* 160, 164307 (2024)

<https://doi.org/10.1063/5.0202588>



29 April 2024 10:03:59



Boost Your Optics and Photonics Measurements

Lock-in Amplifier

Zurich Instruments

Find out more

Boxcar Averager

# Laboratory study of rotationally inelastic collisions of CO<sub>2</sub> at low temperatures

Cite as: *J. Chem. Phys.* **160**, 164307 (2024); doi: [10.1063/5.0202588](https://doi.org/10.1063/5.0202588)

Submitted: 5 February 2024 • Accepted: 21 March 2024 •

Published Online: 23 April 2024



View Online



Export Citation



CrossMark

C. Álvarez,<sup>a),b)</sup>  G. Tejada,<sup>b)</sup>  and J. M. Fernández<sup>b),c)</sup> 

## AFFILIATIONS

Laboratory of Molecular Fluid Dynamics, Instituto de Estructura de la Materia IEM-CSIC, C/Serrano 121, 28006 Madrid, Spain

<sup>a)</sup> Author to whom correspondence should be addressed: [carlosalni01@gmail.com](mailto:carlosalni01@gmail.com)

<sup>b)</sup> URL: <https://www.iem.csic.es/fismol/fdm/>

<sup>c)</sup> [jm.fernandez@csic.es](mailto:jm.fernandez@csic.es)

## ABSTRACT

The rotational relaxation of CO<sub>2</sub> by inelastic collisions has been studied in three supersonic jets. The jets were probed by means of Raman spectroscopy with high spectral and spatial resolutions, measuring the rotational populations and the total number density. The time evolution of the rotational populations was analyzed by means of a kinetic master equation, with the help of the energy-corrected sudden power law to relate the numerous state-to-state rate (STS rates) coefficients. In the thermal range investigated, 60–260 K, the STS rates decrease with increasing temperature and with increasing change in the rotational quantum number. Other quantities of interest for fluid dynamics, such as the rotational collision number, the relaxation cross section, and the bulk viscosity, have been derived from the STS rates.

© 2024 Author(s). All article content, except where otherwise noted, is licensed under a Creative Commons Attribution (CC BY) license (<https://creativecommons.org/licenses/by/4.0/>). <https://doi.org/10.1063/5.0202588>

## I. INTRODUCTION

The kinetics of the excitation and relaxation processes in carbon dioxide (CO<sub>2</sub>) plays a key role in many systems of scientific and technological interest. Some examples are the development of CO<sub>2</sub> lasers,<sup>1</sup> the energy balance in the upper layers of Earth's atmosphere,<sup>2</sup> the entry of spacecrafts into Mars,<sup>3</sup> the modeling of its atmosphere,<sup>4</sup> and the synthesis of fuels by low temperature CO<sub>2</sub> plasmas.<sup>5</sup> Despite these significant implications, reliable experimental data on the myriad of processes involving CO<sub>2</sub> internal relaxation are scarce.

In particular, rotational relaxation of CO<sub>2</sub> has been investigated in the past through sound propagation,<sup>6</sup> thermal transpiration,<sup>7</sup> and time-of-flight analysis of molecular beams.<sup>8</sup> Rotational relaxation rates in excited vibrational states of CO<sub>2</sub> were obtained from the time evolution of the populations of selected rotational energy levels in pump-probe experiments employing laser amplification<sup>9,10</sup> or Raman-IR double resonance.<sup>11,12</sup> The evidence of a vast collection of relaxation channels was acknowledged in these previous studies. Hence, the problem was approached through various methods: retrieving averaged physical quantities such as the relaxation time or collision number,<sup>6–8</sup> grouping all the relaxation processes into a

single one,<sup>9,10</sup> or using fitting laws to relate these processes to a selected subset of them.<sup>11–13</sup>

The sudden expansion of molecular gases in supersonic jets breaks the thermodynamic equilibrium, causing an energy transfer between translational and internal motions. Raman spectroscopy allows an accurate monitoring of the population of both rotational and vibrational energy levels of the molecules, with a spacial resolution of a few micrometer.<sup>14</sup> Thus, probing the supersonic jets by Raman spectroscopy provides accurate measurements of the time evolution of the molecular populations, which can be exploited to investigate the excitation-relaxation kinetics due to inelastic collisions.<sup>15</sup> This has been done in the past for rotationally inelastic collisions of H<sub>2</sub>,<sup>16</sup> N<sub>2</sub>,<sup>17</sup> O<sub>2</sub>,<sup>18</sup> and H<sub>2</sub>O,<sup>19</sup> even opening the possibility of studying different thermodynamic and fluid dynamic quantities in non-equilibrium conditions.<sup>20,21</sup>

The aim of this work was to provide accurate values for the rotational relaxation rate coefficients of CO<sub>2</sub> in its ground vibrational state (0, 0<sup>0</sup>, 0) at low temperatures. This paper is structured as follows: in Sec. II, the experimental setup and the measuring procedure are described. Section III contains the theoretical methodology used for the data analysis. Section IV includes the results, discussion of its validity, and comparisons with the literature. Finally, in

Sec. V, we summarize the conclusions extracted from this work. The detailed information on some of the data treatment is presented in the Appendix.

## II. EXPERIMENTAL

Three jets of CO<sub>2</sub> have been studied in this work, produced in two different instruments, as detailed in the following. The experimental conditions of the jets are listed in Table I. The experimental equipment has been described previously<sup>19</sup> and will only be completed here with details relevant for this work. The supersonic free jets were produced by injecting CO<sub>2</sub> (≥99.7% stated purity) through a Ø400 μm stainless steel airbrush nozzle into an aluminum expansion chamber. A cw laser beam, whose polarization can be rotated by means of a half-wave plate, is sharply focused on a point inside the jet. The Raman scattered radiation is collected at 90° to the jet axis and to the laser beam by using a photographic lens and an achromatic doublet with a total magnification of ×10 and analyzed by means of a spectrometer with a high sensitivity CCD detector cooled by liquid nitrogen.<sup>22</sup> The nozzle, laser focusing optics, and photographic lens installed inside the chamber are moved by remote controlled micro-actuators. In particular, the nozzle's ones allow probing the jet with sub-micrometer accuracy in *xyz*. The expansion chamber is evacuated using a 2000 l/s turbomolecular pump, backed by a roots blower and a rotary pump. A constant gas flow is maintained during the experiment using a Bronkhorst mass flow controller.

Two different apparatus have been used in this study. The first one works at room temperature, and it is suitable for accurately determining the stagnation conditions of the jet. Type K thermocouples are attached to the nozzle and the pre-nozzle chamber to measure the stagnation temperature,  $T_0$ , and the pre-nozzle chamber is directly connected to a capacitance manometer (MKS Baratron) with an accuracy of ±0.01 mbar to measure the stagnation pressure,  $p_0$ . The pressure of the static reference sample was measured using the same Baratron gauge and the background pressure in expansion conditions,  $p_b$ , with a Pirani gauge. The excitation source is an Nd:YVO<sub>4</sub> laser that supplies 8 W at 532 nm. Jet B was measured with this apparatus.

The second apparatus is designed to expand hot gases up to 800 K. To heat the gas, a 210 W Watlow Firerod cartridge with a type K internal thermocouple at its tip is placed axially inside the pre-nozzle chamber, powered through a proportional-integral-derivative (PID) controller with ±1 K accuracy. The pre-nozzle chamber is thermally isolated from the rest of the setup by quartz rods, a water cooled baseplate, and copper radiation shields to protect all the mechanical and optical parts inside the expansion

**TABLE I.** Experimental conditions of the three jets studied in this work produced from a Ø400 μm nozzle and with a molar flow rate of  $Q = 2.53 \times 10^{-4}$  mol/s.

Jet	$T_0$ (K)	$p_0$ (mbar)	$n_0$ (m <sup>-3</sup> )	$p_b$ (mbar)
A	298.0	388.0	$9.43 \times 10^{24}$	0.004
B	294.0	310.0	$7.62 \times 10^{24}$	0.004
C	344.0	422.0	$8.89 \times 10^{24}$	0.005

chamber. These isolation elements also help keep the thermal conditions stable during the experiment. The temperature of the nozzle, pre-nozzle chamber, shields, photographic lens, and laser focusing lens are monitored using type K thermocouples. The gas pressure is measured upstream the nozzle using a piezo-resistive gauge with ±1 mbar accuracy. The pressure of the reference static sample and the background pressure in expansion conditions were measured with another MKS Baratron gauge with accuracy of ±0.001 mbar. The excitation source is an Ar<sup>+</sup> single mode laser that provides 5 W at 514.5 nm. The jets A and C were measured with this apparatus.

In all the expansions, the jet diagnostic protocol was as follows: first, the origin of the *z* scale along the jet axis was set within 0.2 μm by projecting the shadow of the nozzle tip on the spectrometer entrance slit through the previously focused collection optics. Then, static reference Raman spectra of CO<sub>2</sub> at ~40 mbar were recorded at different distances from the nozzle, with a well-known pressure and temperature and exactly the same excitation-collection configuration to be used later in the jet. Next, the jets were produced at the working conditions. For the jet C, the nozzle was heated up to the desired stagnation temperature and, after 2 h of waiting, the setup reached steady thermal conditions. Then, the *z*-scale origin was reset with the shadow of the nozzle to compensate the thermal expansion of the nozzle block. The whole set up is stable for hours. Rotational and vibrational Raman spectra were recorded at numerous discrete points at increasing distances along the jet axis up to 1.0 mm (2.5 nozzle diameters). Examples of both rotational and vibrational spectra in the jet A are shown in Fig. 1. All the jets were checked to be free of condensation by looking for the CO<sub>2</sub> dimer<sup>23</sup> and cluster<sup>14</sup> signatures around the fundamental bands F1 and F2 shown in Fig. 1(b).

## III. METHODOLOGY AND DATA ANALYSIS

The primary physical quantities retrieved from the experiment are the rotational populations,  $P_J$  and the number density  $n$ , which are measured at discrete points along the jet axis. The rotational populations are obtained from the Raman intensity,  $I_J$ , of the  $J \rightarrow J + 2$  rotational transition line [see Fig. 1(a)] as

$$P_J \propto \frac{I_J (2J + 1)(2J + 3)}{\nu^4 (J + 1)(J + 2)}, \quad (1)$$

where  $\nu$  is the wavenumber of the scattered photon. The rotational populations measured in this work were observed to obey to a great extent a Boltzmann distribution. This means that a unique rotational temperature,  $T_R$ , can be measured at each point, with ±1 K of accuracy. In turn, the number densities,  $n$ , at the same points are obtained by summing the intensities of the Q-branches of the vibrational Raman bands [see Fig. 1(b)], weighted by their related polarizability transition moment<sup>24</sup> and compared to those of the aforementioned static sample at a known density. The estimated uncertainty of  $n$  is ±5%. Both the evolution of  $T_R$  and  $n$  along the jet axis were fitted to sigmoid-like functions for better analysis, as explained in the Appendix. The smooth behavior of these functions allows for the precise determination of the gradients  $dT_R/dz$ ,  $dn/dz$ , and  $dP_J/dz$  along the jet axis, within the spanned thermal range of 60–260 K.

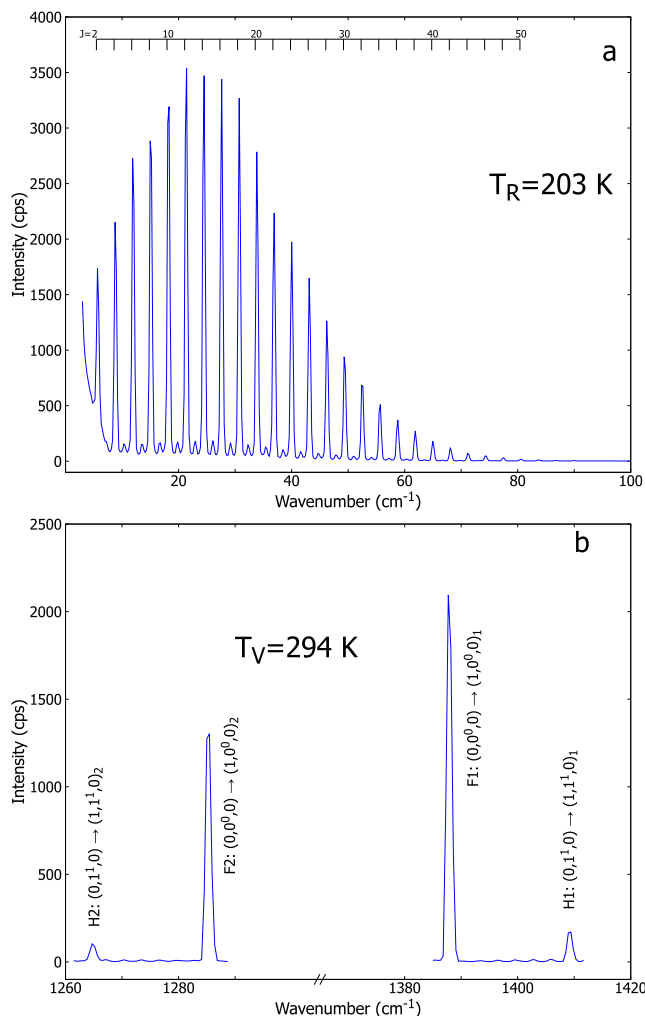


**FIG. 1.** Rotational (a) and vibrational (b) Raman spectra of CO<sub>2</sub>, recorded at  $z = 0.12$  mm in the jet A. The spectral resolutions are  $0.6 \text{ cm}^{-1}$  (a) and  $2.1 \text{ cm}^{-1}$  (b). The vibrational temperature has been obtained from the ratio H1/F1 and H2/F2 of the intensities of the hot to the fundamental bands. The assignments are after Ref. 39.

Other quantities such as the translational temperature  $T_T$  and the flow velocity  $v$  are derived from  $T_R$  and  $n$ . The flow velocity  $v$  is retrieved from the enthalpy conservation along the jet, as explained in the Appendix. The translational temperatures,  $T_T$ , have been obtained using the relaxation equation,

$$\frac{dT_R}{dt} = v \frac{dT_R}{dz} = -\frac{T_R - T_T}{\tau_R}, \quad (2)$$

where  $\tau_R$  is the rotational relaxation time. This method is explained in more detail in the Appendix. Despite its phenomenological origin, this equation has shown to accurately enough describe the breakdown of thermodynamic equilibrium between the translational and rotational motions as long as the ratio  $T_R/T_T < 1.1$ .<sup>25</sup> This condition is fulfilled in all the jets studied in this work since the difference

**TABLE II.** Experimental quantities in the jet A.

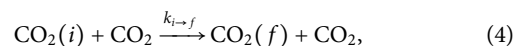
$z$ (mm)	$n$ ( $\text{m}^{-3}$ )	$T_R$ (K)	$T_T$ (K)	$v$ (m/s)	$P_{v=0}$	$P_{v=1}$
0.10	$3.80 \times 10^{24}$	209.6	209.5	343.6	0.928	0.072
0.14	$3.15 \times 10^{24}$	194.4	194.1	372.1	0.928	0.072
0.18	$2.60 \times 10^{24}$	180.0	179.5	397.3	0.928	0.072
0.22	$2.14 \times 10^{24}$	166.5	166.2	418.9	0.929	0.071
0.26	$1.76 \times 10^{24}$	153.9	153.5	438.6	0.928	0.072
0.30	$1.45 \times 10^{24}$	142.4	141.8	456.0	0.928	0.072
0.50	$5.99 \times 10^{23}$	99.4	98.4	515.4	0.928	0.072
0.80	$2.33 \times 10^{23}$	68.9	68.1	553.5	0.931	0.069
1.00	$1.46 \times 10^{23}$	61.1	60.5	563.0	0.935	0.065

$\Delta T = T_R - T_T$  calculated from Eq. (2) reaches a maximum of  $\sim 1$  K. The experimental quantities at representative points of the jet A are presented in Table II, along with the vibrational populations  $P_v$  for the ground ( $v = 0$ ) and the first excited state ( $v = 1$ ). The complete experimental data set for the three jets are given in the tables in the supplementary material, along with the parameters of the fits to sigmoid functions.

The time evolution of the rotational populations  $P_j$  was analyzed by means of a kinetic master equation (MEQ),

$$\frac{dP_i}{dt} = v \frac{dP_i}{dz} = n \sum_{f \neq i} (-P_i k_{i \rightarrow f} + P_f k_{f \rightarrow i}). \quad (3)$$

Here,  $k_{i \rightarrow f}$  are the temperature-dependent state-to-state rate coefficients (STS rates in short) accounting for the rate of the inelastic two-body collision process,



where one of the colliders changes its rotational state from  $i$  to  $f$  and the other remains unchanged. In the absence of three-body collisions and radiative transfers, the MEQ (3) accurately describes the time evolution of the rotational populations along a flow line of the jet due to inelastic collisions. It must be stressed that  $dP_i/dt$ ,  $n$ , and  $P_i$  in MEQ (3) come from the experiment, leaving the rate coefficients,  $k_{i \rightarrow f}$  as the unknowns to be determined.

The number of rotationally inelastic collisional channels  $i \rightarrow f$  of CO<sub>2</sub> at the temperatures of the experiments is too large to invert the MEQ (3) solely from the collected data, so we used the energy-corrected sudden power law (ECS-P) to scale the STS rates involved in the rotational relaxation. The ECS-P is a dynamically based fitting law<sup>26</sup> of the form,

$$k_{i \rightarrow f} = (2f + 1) \exp\left(\frac{E_i - E_{\max}(i,f)}{k_B T_T}\right) \times \sum_{L=|i-f|}^{i+f} \begin{pmatrix} i & f & L \\ 0 & 0 & 0 \end{pmatrix}^2 (2L + 1) \frac{\Omega_{\max}^2(i,f)}{\Omega_L^2} k_{L \rightarrow 0}, \quad (5)$$

**TABLE III.** STS rates ( $10^{-20}$  m<sup>3</sup>/s) for  $i \rightarrow f$  rotational inelastic collisions of CO<sub>2</sub> at 157 K for the jet A.

	$i = 0$	2	4	6	8	10	12	14	16	18	20
$f = 0$	...	4770	1437	686	401	263	186	138	107	85	69
2	23 343	...	10 239	3998	2186	1390	965	710	545	432	351
4	12 043	17 530	...	11 731	4984	2887	1914	1372	1035	811	653
6	7678	9140	15 663	...	12 422	5504	3291	2237	1636	1256	998
8	5271	5870	7817	14 591	...	12 814	5822	3553	2457	1822	1415
10	3726	4024	4883	6971	13 818	...	13 062	6035	3735	2613	1958
12	2657	2822	3268	4210	6340	13 191	...	13 227	6185	3867	2730
14	1889	1986	2240	2736	3700	5828	12 649	...	13 341	6294	3967
16	1331	1390	1541	1825	2331	3288	5392	12 161	...	13 418	6376
18	925	961	1054	1222	1509	2008	2943	5009	11 713	...	13 470
20	632	655	712	814	983	1261	1741	2646	4665	11 293	...

which expresses the STS rates as a function of a basis set of rate coefficients,  $k_{L \rightarrow 0}$ . In Eq. (5),  $\begin{pmatrix} i & f & L \\ 0 & 0 & 0 \end{pmatrix}$  is a Wigner 3J symbol, and  $\Omega_j$  is the adiabatic correction,

$$\Omega_j = \left( 1 + \frac{(E_j - E_{j-2})^2 l_c^2}{24 \hbar^2 \bar{v}_r^2} \right)^{-1}, \quad (6)$$

depending on the  $l_c = 1.73 \text{ \AA}$  scaling length<sup>13</sup> and on the mean relative velocity  $\bar{v}_r$ . The basis of rate coefficients are related to a basic  $k_0$  by the power law,

$$k_{L \rightarrow 0} = k_0 (L(L+1))^{-\alpha}. \quad (7)$$

The  $k_{i \rightarrow f}$  given by Eq. (5) obey the detailed balance,

$$k_{i \rightarrow j} = k_{j \rightarrow i} \frac{2j+1}{2i+1} \times \exp\left(\frac{E_i - E_j}{k_B T_T}\right). \quad (8)$$

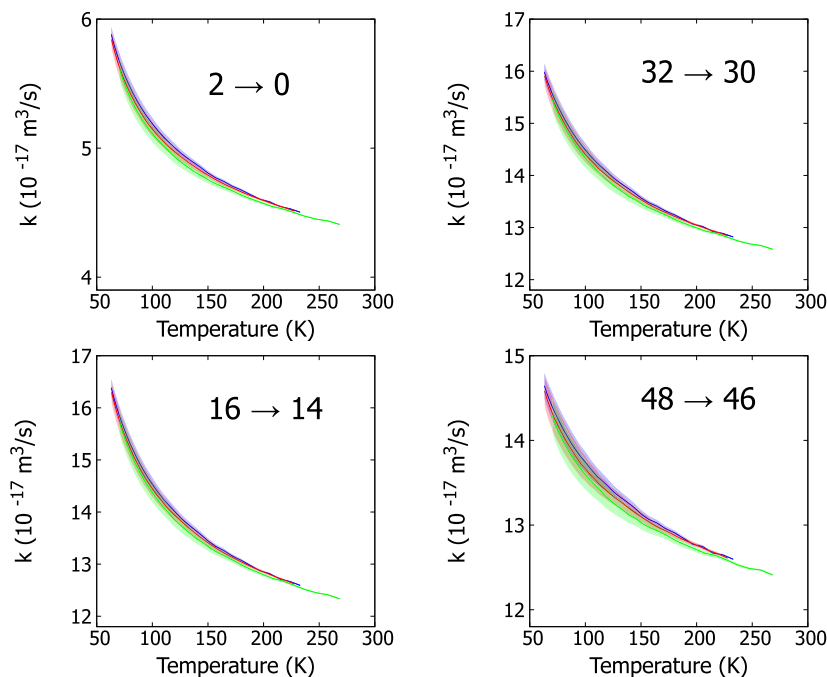


**FIG. 2.** STS rates  $k_{2 \rightarrow 0}$ ,  $k_{16 \rightarrow 14}$ ,  $k_{32 \rightarrow 30}$ , and  $k_{48 \rightarrow 46}$  vs temperatures for the three jets studied in this work (A is in blue, B is in red, and C is in green). The uncertainty of the STS rates is represented by the colored shadow region.

At each  $T_T$ , the experimental  $n$ ,  $P_j$ , and  $dP_j/dt$  were introduced into MEQ (3), with  $k_{i \rightarrow f}$  expressed in terms of the ECS-P parameters  $\alpha$  and  $k_0$  from Eq. (7). These parameters were determined for each jet by a non-linear least-square fit to reproduce the experimental  $dP_j/dt$ .

#### IV. RESULTS AND DISCUSSION

The results obtained from this methodology are shown next. The set of STS rates,  $k_{J \rightarrow J'}$  up to  $J, J' = 80$  are retrieved from the fitted ECS-P coefficients. As an example, STS rates up to  $J = 20$  for jet A at 157 K are presented in Table III. Due to the detailed balance of Eq. (8), the “down”  $k_{J \rightarrow J'}$  ( $J > J'$ ) have a smoother temperature dependence than the “up”  $k_{J' \rightarrow J}$ . Thus, a set of experimental “down” STS rates for various processes with  $\Delta J = 2$ , is shown in Fig. 2 for the three jets studied in this work. Similar behaviors are observed for other values of  $J$  and  $\Delta J$ . In the thermal range spanned in this work, the STS rates grow as the temperature decreases. The uncertainty of  $k_{J \rightarrow J'}$  has been estimated from those of the experimental quantities quoted above, the largest contribution being that of the difference  $\Delta T$  and of the standard deviation of the fits. The estimated  $1\sigma$  uncertainty is, on average, better than 1.5%. It can be seen the good consistency between the three jets, despite having different stagnation conditions or having been measured with independent apparatus. Furthermore, the difference between the same  $k_{J \rightarrow J'}$  for the three jets is smaller than the estimated uncertainty.

This points toward the robustness of the experiment and the data analysis. In particular, the relaxation Eq. (2) accurately describes the difference  $\Delta T$  between the translational and rotational temperatures, at least within the temperature range analyzed.

The “down” STS rates for processes with  $\Delta J = 2, 4$ , and  $6$  at 157 K for jet A are shown in Fig. 3, with similar trends for larger  $\Delta J$ . For all  $\Delta J$ , the STS rates grow with  $J$  until reaching a smooth maximum and then decreasing slowly. For  $\Delta J = 2$ , this maximum is reached at  $J = 24$ . Despite the dominance of the STS rates with

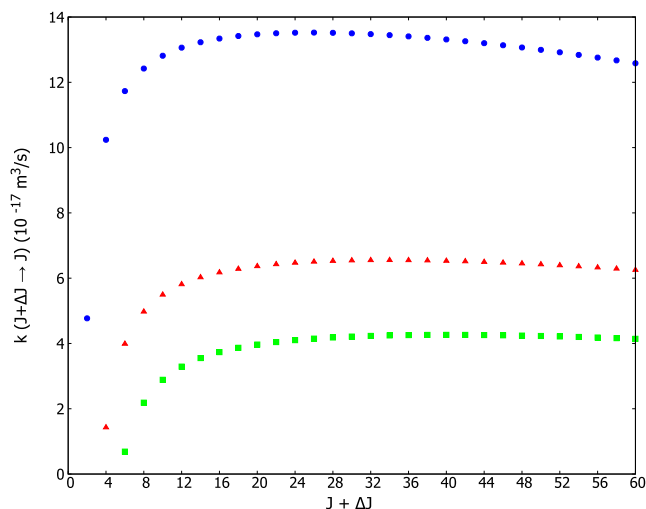


**FIG. 3.** STS rates for “down” inelastic collisions with  $(J + \Delta J) \rightarrow J$  with  $\Delta J = 2$  (the blue circle), 4 (the red triangle), and 6 (the green square) for different rotational energy levels in the jet A at  $T = 157$  K.

$|\Delta J| = 2$ , collisions with larger  $|\Delta J|$  cannot be neglected in the kinetic analysis through MEQ (3) to properly describe the rotational relaxation in the jets.

The  $k_{J \rightarrow J'}$  for processes starting from the rotational level  $J = 16$  are shown in Fig. 4 for jet A at two different temperatures. It can be seen how the STS rates diminish with increasing  $|\Delta J|$ , with this effect being more pronounced as the temperature is lower: at  $T = 150$  K, the STS rates with  $\Delta J > 14$  are negligible, while at  $T = 75$  K, the same is achieved for  $\Delta J > 10$ . These limits roughly correspond to a change in the rotational energy of the order of the kinetic energy of the bath. Furthermore, the STS rates for “down” processes shown in Fig. 4 decrease with increasing temperature, as shown in Fig. 2, while the ratio between the “up” and “down” STS rates grows with the temperature due to the detailed balance of Eq. (8).

From the MEQ (3), the rotational relaxation time can be calculated as<sup>25</sup>

$$\tau_R^{-1} = \frac{n(\beta B)^2}{T_R T_T} \sum_{i>f} \sum_f [i(i+1) - f(f+1)]^2 k_{i \rightarrow f} P_i, \quad (9)$$

where  $B = 0.39022 \text{ cm}^{-1}$  is the rotational constant of  $\text{CO}_2$  and  $\beta = 1.438765 \text{ cm K}$ . This rotational relaxation time has been compared to that used in Eq. (2) to calculate the translational temperature. Both rotational relaxation times differ by less than 1% for the three jets, as shown in Fig. 5, proving the self-consistency of the method, and that we are safely within the relaxation equation approximation.

To our knowledge, no experimental STS rates for rotational relaxation in  $\text{CO}_2$  below room temperature have been reported previously. Hartmann and Boulet calculated some STS rates at 296 K<sup>13</sup> employing the ECS approximation. Although being of the same order of magnitude, their STS rates are systematically larger than ours. For example, for  $k_{16 \rightarrow 14}$ , they reported  $1.45 \times 10^{-16} \text{ m}^3/\text{s}$  at 296 K vs  $1.24 \times 10^{-16} \text{ m}^3/\text{s}$  at 258 K obtained here. That difference can be due to the fact that their STS rates were calculated with the

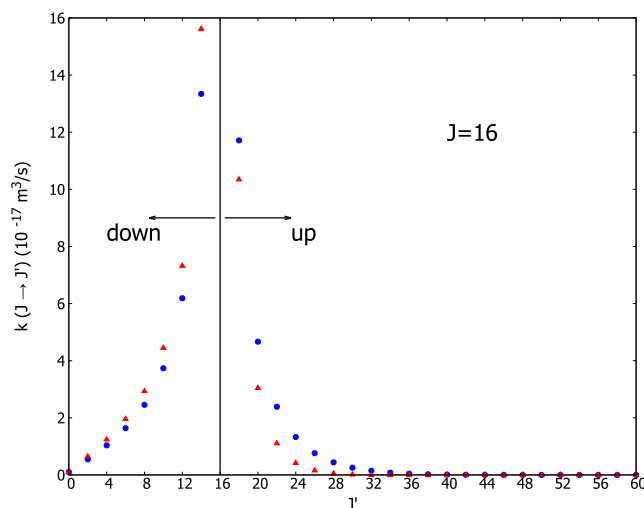


**FIG. 4.** STS rates for inelastic collisions  $J \rightarrow J'$  departing from  $J = 16$  at  $T = 150$  K (the blue circles) and  $T = 75$  K (the red triangles).

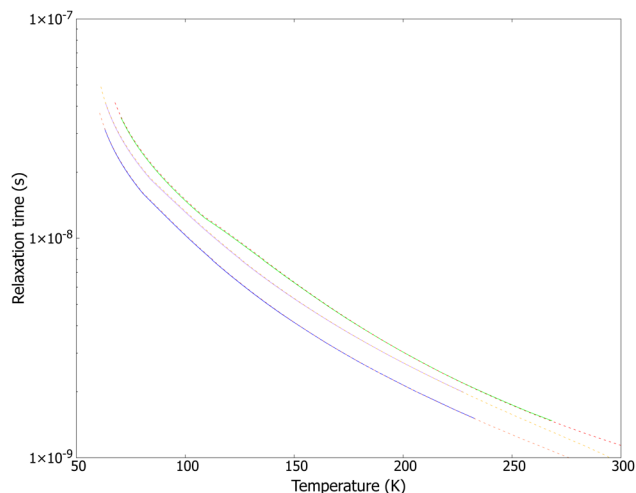


**FIG. 5.** CO<sub>2</sub> rotational relaxation time,  $\tau_R$ , for the three jets studied in this work (A is in blue, B is in red, and C is in green) vs temperature. The solid lines, calculated from STS rates by means of Eq. (9); the dashed lines, calculated from Eq. (2), as explained in the Appendix.

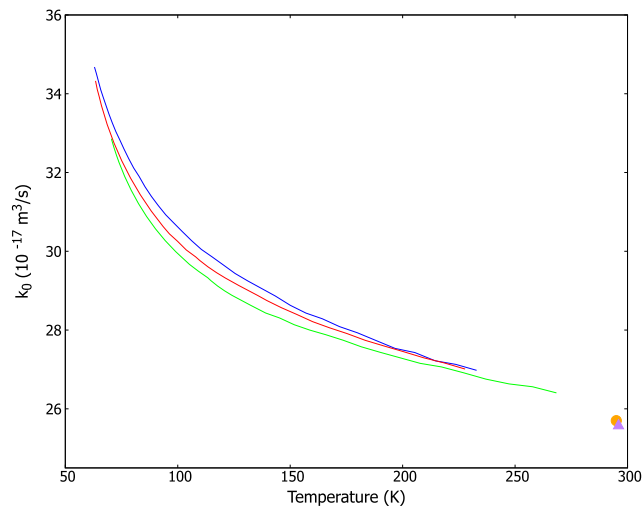


**FIG. 6.** ECS basic rate,  $k_0$  of Eq. (7) vs temperature for the three jets studied in this work (A is in blue, B is in red, and C is in green). The circle is from Ref. 11 and the triangle from Ref. 13.

ECS parameters derived from line broadening coefficients, not from more accurate time resolved relaxation experiments.

The experimental rotational relaxation rates  $k_J = \sum_i k_{J \rightarrow i}$  for selected  $J$  levels in excited vibrational states have been reported from the time-resolved pump-probe experiments at room temperature.<sup>9–11</sup> Cheo and Abrams<sup>9</sup> reported  $k_J = 3.4 \times 10^{-16} \text{ m}^3/\text{s}$  for  $J = 19$  of the  $(0, 0^0, 1)$  vibrational state in the saturation recovery experiments of a CO<sub>2</sub> lasing line, while Jacobs, Pettipiece, and Thomas<sup>10</sup> measured  $k_{19} = 4.0 \times 10^{-16} \text{ m}^3/\text{s}$  in a better resolved experiment. From our STS rates, we obtained  $k_J = 5.3 \times 10^{-16} \text{ m}^3/\text{s}$  for comparable  $J = 18$  of the ground state  $(0, 0^0, 0)$  at 258 K. In turn, Millot and Roche<sup>11</sup> measured  $k_J$  for  $J = 16\text{--}32$  within the  $(0, 2^0, 0)$  vibrational state in the experiments of Raman-IR double resonance. Their relaxation rates range from  $k_{16} = 6.0 \times 10^{-16}$  to  $k_{32} = 4.7 \times 10^{-16} \text{ m}^3/\text{s}$  at 295 K. From our STS rates, we obtained  $k_{16} = 5.32 \times 10^{-16}$  and  $k_{32} = 5.34 \times 10^{-16} \text{ m}^3/\text{s}$  at 258 K for the ground vibrational state  $(0, 0^0, 0)$ . These results are consistent despite coming from different experiments at different temperatures and probing different vibrational states.

Since some of the experiments mentioned above also used the ECS law to scale the STS rates, a comparison of some of the ECS parameters is illustrative. In particular,  $k_0$  for the three jets studied in this work is shown in Fig. 6, along with those from the literature.<sup>11,13</sup> The basic rates,  $k_0$ , decrease with increasing temperature, consistent with the thermal behavior of the individual STS rates shown in Fig. 2, and tend to those of the literature at room temperature. The exponent  $\alpha$  of the power law in Eq. (7) is of the order of  $\sim 0.9$  in all cases.

It is interesting to note that this temperature behavior of STS rates for rotationally inelastic collisions does not seem to be universal. For previous molecules studied in our laboratory, such as H<sub>2</sub>,<sup>16</sup> N<sub>2</sub>,<sup>17</sup> or O<sub>2</sub>,<sup>18</sup> the “down” STS rates increased with temperature in their investigated thermal ranges. On the contrary, STS rates in acetylene are larger at 155 K<sup>27</sup> than at room temperature,<sup>28</sup> in line

with the observed behavior of CO<sub>2</sub> in the present work. Furthermore, related collisional STS rates, like those involved in the line mixing of IR absorption lines of CO<sub>2</sub> perturbed by N<sub>2</sub> and O<sub>2</sub>,<sup>29</sup> show the same temperature behavior as CO<sub>2</sub> in the present work.

Other quantities often used in the literature to characterize the rotational relaxation, such as the rotational collision number  $Z_R$ <sup>30</sup> and the rotational effective cross section  $\sigma_R$ , can be derived from the STS rates via the relaxation time  $\tau_R$ .<sup>31</sup> These quantities are related by

$$Z_R = \tau_R f = \frac{\pi d^2}{\sigma_R}, \quad (10)$$

where  $f$  is the gas-kinetic collision frequency<sup>30,32</sup> given in Eq. (A4) and  $d$  is the effective collisional diameter. Unlike  $\tau_R$ , which depends on the temperature and density,  $Z_R$  and  $\sigma_R$  are only temperature dependent and thus, better suited for comparison between different experiments. The values of  $\sigma_R$  for the three jets studied in this work are shown in Fig. 7. It can be seen that there is good agreement of this quantity for the three jets despite their different stagnation conditions, unlike what happened for  $\tau_R$ , as shown in Fig. 5. Gallagher and Fenn<sup>8</sup> reported  $Z_R = 2.5$  at room temperature from molecular beam experiments, referred to a collisional diameter of  $d = 3.95 \text{ \AA}$ . The corresponding  $\sigma_R = 20 \text{ \AA}^2$  is shown in Fig. 7, where a trend from our  $\sigma_R$  to the value at room temperature can be appreciated.

Rotational relaxation of CO<sub>2</sub> below room temperature has been studied theoretically,<sup>33,34</sup> although not in terms of STS rates. Cameron and Harland<sup>33</sup> performed a Monte Carlo calculation of the rotational collision number  $Z_R$  of CO<sub>2</sub> between 40 and 300 K. The qualitative behavior of their  $Z_R$  with temperature is similar to ours. However, these authors used  $(T_R - T_e)$ , with  $T_e = (3T_T + 2T_R)/5$  in their relaxation equation, instead of  $(T_R - T_T)$ . Thus, their  $\tau_R$  and  $Z_R$  are expected to be roughly halved with respect to those obtained here from Eq. (2). With this conversion, their  $Z_R$  (e.g.,  $Z_R \sim 2.5$  at 150 K) becomes comparable to ours ( $Z_R = 2.6$ ).

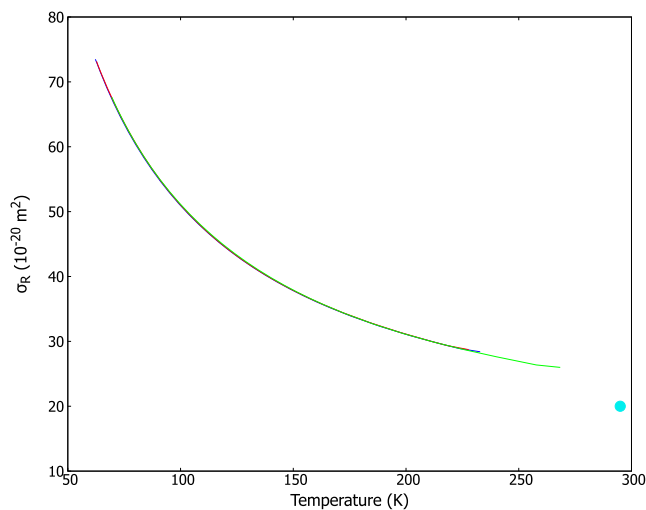


**FIG. 7.** Rotational effective cross section,  $\sigma_R$  of  $\text{CO}_2$  vs temperature for the three jets studied in this work (A is in blue, B is in red, and C is in green). The circle is from Ref. 8.

Kustova *et al.*<sup>34</sup> focused on the effect of the bulk viscosity in the internal relaxation of  $\text{CO}_2$ . The bulk, or second, viscosity can be understood as a macroscopic quantity in fluid dynamics that takes into account all the internal relaxation processes that work to restore the thermodynamic equilibrium when a sudden change in volume takes place.<sup>35</sup> Typically, these processes are so rapid that the bulk viscosity is negligible. However, in a compression or expansion fast enough like in supersonic jets, or in molecules with long relaxation times, it can become comparable to the shear viscosity,  $\mu$ . The rotational contribution to the bulk viscosity can be modeled as<sup>31,34</sup>

$$\eta_R = \frac{k_B^2 c_R}{c_V^2} T_T n \tau_R, \quad (11)$$

where  $c_R$  and  $c_V$  are the rotational and the total heat capacity of  $\text{CO}_2$  per molecule. As has been shown previously, the rotational populations of the jets studied in this work obey a Boltzmann distribution, so  $c_R = k_B$ . On the other hand, since the populations  $P_v$  of the excited vibrational level  $v = 1$  are small and almost constant (see Table II), we neglect the vibrational contribution to the internal heat capacity, as was also done in comparable molecular beam experiments.<sup>8</sup> So, the total heat capacity is  $c_V = 3/2k_B + c_R$ . The bulk viscosity,  $\eta$ , is usually given relative to the shear viscosity  $\mu$ , which has been modeled as  $\mu = \mu_{ref} (T_T/T_{ref})^\omega$ , where  $\mu_{ref} = 1.38 \times 10^{-5}$  Pa s,  $T_{ref} = 273$  K, and  $\omega = 0.93$ .<sup>36</sup> The ratio between the bulk and shear viscosities,  $\eta/\mu$ , is shown in Fig. 8 for the three jets studied in this work. It can be seen that the ratio  $\eta/\mu$  is less than 0.5 in the temperature range studied in this work. This is consistent with the measurements taken at room temperature from Brillouin light scattering,<sup>37</sup> and the calculations by Kustova *et al.*<sup>34</sup> disregarding the vibrational contribution.

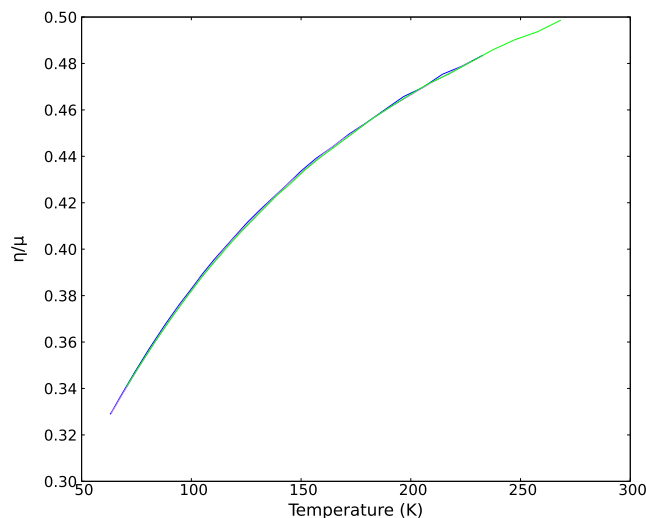


**FIG. 8.** Ratio between the bulk  $\eta$  and shear  $\mu$  viscosities of  $\text{CO}_2$  vs temperature for the three jets studied in this work (A is in blue, B is in red, and C is in green).

Finally, for the practical use of our STS rates at any temperature between 60 and 260 K, we propose a model of the ECS-P parameters with the temperature as

$$k_0(T) = a \times \exp(b/T), \quad (12)$$

where  $a = (2.464 \pm 0.004) \times 10^{-16}$  m<sup>3</sup>/s,  $b = (20.830\,169 \pm 0.164\,792)$  K, and

$$\alpha(T) = a - T/b + (T/c)^2 - (T/d)^3 \quad (13)$$

with  $a = (0.992\,198 \pm 0.002\,531)$ ,  $b = (5276.462\,000 \pm 1607.690\,981)$  K,  $c = (703.656\,773 \pm 68.569\,101)$  K, and  $d = (600.982\,086 \pm 35.718\,456)$  K. The root mean squared error (RMSE) of the fits in Eqs. (12) and (13) are 0.012 592 and 0.000 919, respectively. With these expressions and the ECS-P law in Eqs. (5)–(7), the STS rates can be calculated in the thermal range of 60–260 K, the difference between the experimental and modeled STS rates being less than 1%.

## V. CONCLUDING REMARKS

The time evolution of the populations  $dP_J/dt$  of the rotational levels of  $\text{CO}_2$  has been measured in three supersonic jets by means of Raman spectroscopy with high-spatial resolution. These time derivatives have been analyzed with a master equation (MEQ) employing the ECS-P scaling law to relate the many STS rates involved in each  $dP_J/dt$ , along with a relaxation equation to determine the translational temperature. A complete set of STS rates for  $\Delta J = \text{even up to } J = 80$  has been obtained between 60 and 260 K, which reproduces the observed  $dP_J/dt$  within 1%. For practical use, a modeling of the ECS-P parameters is given.

The STS rates obtained in this work confirm the propensity in favor of smaller  $\Delta J$ ,  $\Delta J = 2$  being dominant, although larger  $\Delta J$  cannot be disregarded for satisfactory analysis of the collisional kinetics. This work also shows that the relaxation equation accurately



describes the difference between the rotational and translational temperatures within the spanned thermal range.

This work shows the versatility of supersonic jets when combined with Raman spectroscopy. This technique allows the study of molecular collisions in the gas phase down to temperatures out of reach for static techniques. A great number of molecular and fluid dynamic quantities can be retrieved from the experimental measurements. Furthermore, several quantities have been obtained from the STS rates, such as the rotational collision number  $Z_R$ , the rotational relaxation effective cross section  $\sigma_R$ , and the rotational contribution to the bulk viscosity  $\eta_R$ , often employed to characterize the rotational relaxation in computational fluid dynamics. The results of this work are consistent with the few comparable results found in the literature.

It is worth mentioning that the inelastic collision represented in Eq. (4) is truly a four-index process, where both colliding molecules can change their rotational energy. However, this work proves that the collisional kinetics can be satisfactorily interpreted with a two-index approximation, as long as the number of internal states is large enough.

The STS rates for rotationally inelastic collisions of  $\text{CO}_2$  obtained in this work, decrease with increasing temperature, unlike other small molecules studied previously. Although the ultimate cause for this thermal behavior lies within the inelastic cross sections due to the different intermolecular potentials, a theoretical rationale of this in terms of such potential and the collision energy would be desirable.

Finally, it is expected to extent the present methodology to higher temperatures where the vibrational contribution could play a more significant role, either as direct vibrational relaxation or its effect on the rotational relaxation.

## DEDICATION

In Memoriam Salvador Montero (1943–2022), founder of the Laboratory of Molecular Fluid Dynamics.

## SUPPLEMENTARY MATERIAL

See the supplementary material for three files with the complete datasets for the jets A, B and C. The files include: (i) the experimental conditions of the jets, (ii) the fitting functions of  $n$  and  $T_R$  with their parameters, and (iii) the tables with the experimental and fitted number densities, the experimental and fitted rotational temperatures, the translational temperatures, the flow velocities, and the experimental vibrational populations at the discrete measured  $z$  points.

## ACKNOWLEDGMENTS

We thank Salvador Montero (1943–2022), founder of the Laboratory of Molecular Fluid Dynamics, for his knowledge, expertise, and inspiration, which made this work, and others to come, possible.

This work has been supported by the Spanish MCIN/AEI/10.13039/501100011033/and by the European

Union NextGenerationEU/PRTR through Grant Nos. PID2021-123752NB-I00 and TED2021-129619B-I00. C.A. acknowledges the Spanish MCIN/AEI for a predoctoral Grant No. PRE2018-085960. This work has received funding from the European Union's Horizon 2020 research and innovation programme under the Marie Skłodowska-Curie Grant Agreement No. 872081.

## AUTHOR DECLARATIONS

### Conflict of Interest

The authors have no conflicts to disclose.

### Author Contributions

**C. Álvarez:** Data curation (equal); Formal analysis (equal); Investigation (equal); Methodology (equal); Writing – original draft (equal); Writing – review & editing (equal). **G. Tejeda:** Conceptualization (equal); Data curation (equal); Funding acquisition (equal); Investigation (equal); Methodology (equal); Supervision (equal); Writing – review & editing (equal). **J. M. Fernández:** Conceptualization (equal); Data curation (equal); Funding acquisition (equal); Investigation (equal); Methodology (equal); Supervision (equal); Writing – review & editing (equal).

## DATA AVAILABILITY

The data that support the findings of this study are available within the article and its supplementary material.

## APPENDIX: DATA TREATMENT

The number density,  $n$ , and the rotational populations,  $P_j$ , were measured directly in the experiment at discrete  $z$  points. Rotational temperatures  $T_R$  were obtained by fitting the rotational populations to a Boltzmann distribution using the rigid rotor approximation. To get a continuous description of the flow quantities, the experimental  $T_R$  and  $n$  were fitted to sigmoid-like functions of the form,

$$Y(z) = c + (Y_0 - c) \exp(-b(z - z_0)^a), \quad (\text{A1})$$

where  $z_0$  is the origin of the expansion;  $Y_0$  is the stagnation value of  $Y$ ; and  $a$ ,  $b$ , and  $c$  are parameters to be fitted. The correlation coefficient of all these fits was  $R^2 > 0.999$ . The best fit parameters for the raw experimental data of the three jets are provided in the tables in the supplementary material.

The flow velocity  $v$  has been retrieved through the enthalpy conservation along the jet axis in the absence of condensation,

$$v^2(z) = \frac{1}{m} [5k_B(T_0 - T_T(z)) + 2(H_0 - H(z))], \quad (\text{A2})$$

where  $m$  is the molecular mass of  $\text{CO}_2$  and subscript 0 refers to the stagnation conditions. The rotational and vibrational enthalpy,  $H = H_R + H_V$ , has been calculated from the molecular populations as  $H_\alpha = k_B \sum_i P_i \epsilon_i$ , where  $\epsilon_i$  is the energy of the rotational ( $\alpha = R$ ) or vibrational ( $\alpha = V$ ) energy levels, expressed in kelvin.

The rotational relaxation time  $\tau_R$  has been calculated via the rotational collision number  $Z_R$  and the gas-kinetic collision frequency  $f$ , as  $\tau_R = Z_R/f$ . The rotational collision number has been modeled<sup>38</sup> as

$$Z_R = Z^\infty \left[ 1 + \frac{\pi^{3/2}}{2} \left( \frac{b}{T_T} \right)^{1/2} + \left( \frac{\pi^2}{4} + \pi \right) \left( \frac{b}{T_T} \right) \right]^{-1}, \quad (\text{A3})$$

where  $Z^\infty = 17.9$  and  $b = 100$  K for  $\text{CO}_2$ .<sup>14</sup> The gas-kinetic collision frequency is<sup>30,32</sup>

$$f = 4nd^2 \sqrt{\frac{\pi k_B T_T}{m}}, \quad (\text{A4})$$

where  $d = 5.56$  Å is the effective collisional diameter for  $\text{CO}_2$ .<sup>36</sup>

To obtain  $T_T$ , an iterative process was carried out at each  $z$  point using  $T_R$  as the starting value for  $T_T$  to calculate  $v$ ,  $f$ ,  $Z_R$ , and  $\tau_R$ . With these quantities, a new value of  $T_T$  was calculated, and the process was repeated until convergence. Few iterations were necessary for  $T_T$  to converge.

## REFERENCES

- R. L. Taylor and S. Bitterman, "Survey of vibrational relaxation data for processes important in the  $\text{CO}_2$ - $\text{N}_2$  laser system," *Rev. Mod. Phys.* **41**, 26 (1969).
- B. Funke, M. Lopez-Puertas, M. Garcia-Comas, M. Kaufmann, M. Hopfner, and G. P. Stiller, "GRANADA: A generic radiative transfer and non-LTE population algorithm," *J. Quant. Spectrosc. Radiat. Transfer* **113**, 1771 (2012).
- I. Armenise, P. Reynier, and E. Kustova, "Advanced models for vibrational and chemical kinetics applied to mars entry aerothermodynamics," *J. Thermophys. Heat Transfer* **30**, 705 (2016).
- S. Maurice, B. Chide, N. Murdoch, R. D. Lorenz *et al.*, "In situ recording of Mars soundscape," *Nature* **605**, 653 (2022).
- A. George, B. Shen, M. Craven, Y. Wang, D. Kang, C. Wu, and X. Tu, "A review of non-thermal plasma technology: A novel solution for  $\text{CO}_2$  conversion and utilization," *Renewable Sustainable Energy Rev.* **135**, 109702 (2021).
- R. Holmes, G. R. Jones, and R. Lawrence, "Rotational relaxation in carbon dioxide and nitrous oxide," *J. Chem. Phys.* **41**, 2955 (1964).
- A. P. Malinauskas, J. W. Gooch, B. K. Annis, and R. E. Fuson, "Rotational collision numbers of  $\text{N}_2$ ,  $\text{O}_2$ ,  $\text{CO}$ , and  $\text{CO}_2$  from thermal transpiration measurements," *J. Chem. Phys.* **53**, 1317 (1970).
- R. J. Gallagher and J. B. Fenn, "Relaxation rates from time of flight analysis of molecular beams," *J. Chem. Phys.* **60**, 3487 (1974).
- P. K. Cheo and R. L. Abrams, "Rotational relaxation rate of  $\text{CO}_2$  laser levels," *Appl. Phys. Lett.* **14**, 47 (1969).
- R. R. Jacobs, K. J. Pettipiece, and S. J. Thomas, "Rotational relaxation rate constants for  $\text{CO}_2$ ," *Appl. Phys. Lett.* **24**, 375 (1974).
- G. Millot and C. Roche, "State-to-state vibrational and rotational energy transfer in  $\text{CO}_2$  gas from time-resolved Raman-infrared double resonance experiments," *J. Raman Spectrosc.* **29**, 313 (1998).
- A. Deroussiaux and B. Lavorel, "Vibrational and rotational collisional relaxation in  $\text{CO}_2$ -Ar and  $\text{CO}_2$ -He mixtures studied by stimulated Raman-infrared double resonance," *J. Chem. Phys.* **111**, 1875 (1999).
- J. M. Hartmann and C. Boulet, "Quantum and classical approaches for rotational relaxation and nonresonant laser alignment of linear molecules: A comparison for  $\text{CO}_2$  gas in the nonadiabatic regime," *J. Chem. Phys.* **136**, 184302 (2012).
- B. Maté, G. Tejada, and S. Montero, "Raman spectroscopy of supersonic jets of  $\text{CO}_2$ : Density, condensation, and translational, rotational, and vibrational temperatures," *J. Chem. Phys.* **108**, 2676 (1998).
- S. Montero, B. Maté, G. Tejada, J. Fernández, and A. Ramos, "Raman studies of free jet expansion (diagnostics and mapping)," in *Atomic and Molecular Beams: The State of the Art 2000*, edited by R. Campargue (Springer, Berlin, 2001), pp. 295–306.
- S. Montero, G. Tejada, and J. M. Fernández, "Laboratory study of rate coefficients for  $\text{H}_2$ : $\text{H}_2$  inelastic collisions between 295 and 20 K," *Astrophys. J., Suppl. Ser.* **247**, 14 (2020).
- J. P. Fonfría, A. Ramos, F. Thibault, G. Tejada, J. M. Fernández, and S. Montero, "Inelastic collisions in molecular nitrogen at low temperature ( $2 \leq T \leq 50$  K)," *J. Chem. Phys.* **127**, 134305 (2007).
- J. Perez-Rios, G. Tejada, J. M. Fernández, M. I. Hernández, and S. Montero, "Inelastic collisions in molecular oxygen at low temperature ( $4 \leq T \leq 34$  K). Close-coupling calculations versus experiment," *J. Chem. Phys.* **134**, 174307 (2011).
- G. Tejada, E. Carmona-Novillo, E. Moreno, J. M. Fernández, M. I. Hernández, and S. Montero, "Laboratory study of rate coefficients for  $\text{H}_2\text{O}$ :He inelastic collisions between 20 and 120 K," *Astrophys. J., Suppl. Ser.* **216**, 3 (2015).
- S. Montero, "Temperature and entropy in supersonic free jets," *Phys. Fluids* **25**, 056102 (2013).
- S. Montero, "Molecular description of steady supersonic free jets," *Phys. Fluids* **29**, 096101 (2017).
- G. Tejada, J. M. Fernández-Sánchez, and S. Montero, "High-performance dual Raman spectrometer," *Appl. Spectrosc.* **51**, 265 (1997).
- A. Vigin, F. Huisken, A. Pavlyuchko, L. Ramonat, and E. G. Tarakanova, "Identification of the  $(\text{CO}_2)_2$  dimer vibrations in the  $\nu_1, 2\nu_2$  region: Anharmonic variational calculations," *J. Mol. Spectrosc.* **209**, 81 (2001).
- G. Tejada, B. Maté, and S. Montero, "Overtone Raman spectrum and molecular polarizability surface of  $\text{CO}_2$ ," *J. Chem. Phys.* **103**, 568 (1995).
- S. Montero, "Raman spectroscopy experiments on Boltzmann collision integral in supersonic jets," *AIP Conf. Proc.* **1084**, 3 (2008).
- T. A. Brunner and D. Pritchard, "Fitting laws for rotationally inelastic collisions," in *Dynamics of the Excited State, Advances in Chemical Physics Vol. 50*, edited by K. P. Lawley (John Wiley and Sons, Ltd., 1982), Chap. 9, pp. 589–641.
- J. Domenech, R. Martinez, A. Ramos, and D. Bermejo, "Direct determination of state-to-state rotational energy transfer rate constants via a Raman-Raman double resonance technique: *ortho*-acetylene in  $\nu_2 = 1$  at 155 K," *J. Chem. Phys.* **132**, 154303 (2010).
- R. Dopheide, W. Cronrath, and H. Zacharias, "Rotational energy transfer in vibrationally excited acetylene  $X^1\Sigma_g(v''_2 = 1, J'')$ :  $\Delta J$  propensities," *J. Chem. Phys.* **101**, 5804 (1994).
- R. Rodrigues, K. W. Jucks, N. Lacombe, G. Blanquet, J. Walrand, W. Traub, B. Khalil, R. le Doucen, A. Valentin, C. Camy-peyret, L. Bonamy, and J.-M. Hartmann, "Model, software, and database for computation of line-mixing effects in infrared Q branches of atmospheric  $\text{CO}_2$ -I. Symmetric isotopomers," *J. Quant. Spectrosc. Radiat. Transfer* **61**, 153 (1999).
- J. D. Lambert, *Vibrational and Rotational Relaxation in Gases* (Clarendon Press, Oxford, 1977).
- S. Montero and J. Perez-Rios, "Rotational relaxation in molecular hydrogen and deuterium: Theory versus acoustic experiments," *J. Chem. Phys.* **141**, 114301 (2014).
- P. Atkins and J. de Paula, *Physical Chemistry*, 8th ed. (W. H. Freeman and Company, New York, 2006).
- B. R. Cameron and P. W. Harland, "Monte Carlo calculation of rotational relaxation in small molecules," *J. Chem. Soc., Faraday Trans.* **89**, 3517 (1993).
- E. Kustova, M. Mekhonoshina, and A. Kosareva, "Relaxation processes in carbon dioxide," *Phys. Fluids* **31**, 046104 (2019).
- L. Landau and E. Lifshitz, *Fluid Mechanics*, 2nd ed. (Pergamon Press, Oxford, 1987).
- G. Bird, *Molecular Gas Dynamic and the Direct Simulation of Gas Flows*, 1st ed. (Oxford Engineering Science Series, New York, 1994).
- Y. Wang, W. Ubachs, and W. van de Water, "Bulk viscosity of  $\text{CO}_2$  from Rayleigh-Brillouin light scattering spectroscopy at 532 nm," *J. Chem. Phys.* **150**, 154502 (2019).
- J. G. Parker, "Rotational and vibrational relaxation in diatomic gases," *Phys. Fluids* **2**, 449 (1959).
- J. M. Fernandez, A. Punge, G. Tejada, and S. Montero, "Quantitative diagnostics of a methane/air mini-flame by Raman spectroscopy," *J. Raman Spectrosc.* **37**, 175 (2006).